

# Experimental Investigation of the Dynamic Elastic Modulus and Vibration Damping in MoSi<sub>2</sub>-30%Si<sub>3</sub>N<sub>4</sub> as a Function of Temperature

G.T. Olsen, A. Wolfenden, and M.G. Hebsur

(Submitted 21 May 1999; in revised form 8 September 1999)

The dynamic elastic modulus,  $E$ , and vibration damping of molybdenum disilicide (MoSi<sub>2</sub>) with 30% volume addition of silicon nitride (Si<sub>3</sub>N<sub>4</sub>) were measured at varying temperatures using the piezoelectric ultrasonic composite oscillator technique (PUCOT). The value of the elastic modulus of the composite was observed to decrease as temperature,  $T$ , was increased. The value of  $dE/dT$  of MoSi<sub>2</sub> was determined to be  $-0.03$  GPa/K. The vibration damping of MoSi<sub>2</sub>-30%Si<sub>3</sub>N<sub>4</sub> increased as temperature was increased, with an effective activation energy of  $0.076$  eV/atom. This was an average over the entire temperature range, but two distinct slopes were observed in the plot of damping versus inverse temperature.

**Keywords** ceramics, molybdenum disilicide, silicon nitride, Young's modulus, damping

## 1. Introduction

### 1.1 Interest in MoSi<sub>2</sub>-30%Si<sub>3</sub>N<sub>4</sub> and Applications

Molybdenum disilicide (MoSi<sub>2</sub>) is an intermetallic compound that is promising as a structural material for aerospace applications due to a high melting point (2030 °C), excellent high-temperature oxidation resistance, relatively low density ( $\sim 6.2$  g/cm<sup>3</sup>), high thermal conductivity, and good machinability. Silicon nitride (Si<sub>3</sub>N<sub>4</sub>) is a ceramic that, when added to MoSi<sub>2</sub> in particulate form, significantly increases the low-temperature oxidation resistance of the material.<sup>[1,2]</sup>

### 1.2 Objective

This study was concerned with the measurement of Young's modulus and the vibration damping characteristics of MoSi<sub>2</sub>-30%Si<sub>3</sub>N<sub>4</sub> with increasing temperature. Young's modulus and vibration damping were measured using the piezoelectric ultrasonic composite oscillator technique (PUCOT). Elastic modulus and vibration damping are both important design parameters for applications of materials.

## 2. Materials

Samples of MoSi<sub>2</sub>-30%Si<sub>3</sub>N<sub>4</sub> measuring 3 by 5 by 25 mm were used. The MoSi<sub>2</sub>-30%Si<sub>3</sub>N<sub>4</sub> was chosen due to its resistance to low-temperature oxidation, also known as pesting. Consolidation of the MoSi<sub>2</sub> and Si<sub>3</sub>N<sub>4</sub> powders was done by vacuum hot pressing. Full density was then achieved by hot isostatic pressing.<sup>[2]</sup>

G.T. Olsen and A. Wolfenden, Mechanical Engineering Department, Texas A&M University, College Station, TX 77843; and M.G. Hebsur, John H. Glenn Research Center, NASA Lewis Field, Cleveland, OH 44135.

## 3. Experimental Procedure

### 3.1 Young's Modulus and Vibration Damping at Elevated Temperature

Dynamic elastic modulus,  $E$ , and vibration damping,  $Q^{-1}$ , were measured at 162 kHz using the PUCOT. The PUCOT assembly (Fig. 1) consisted of two  $\alpha$ -quartz piezoelectric crystals designed to vibrate in the longitudinal mode by application of an alternating voltage to the drive crystal,  $D$ . A fused quartz spacer rod,  $Q$ , was attached to the bottom of the gauge crystal, and this arrangement was used to tune the rod for use at a specific temperature. The free end of the rod was placed into a furnace, and the temperature was increased until the period of the drive-gauge rod system was the same as that for the drive-gauge only arrangement. By placing the specimen,  $S$ , on the end of the tuned rod, the effect of the specimen on the resonant period of the system was similar to that upon the drive-gauge only. The resonant period and the output voltage were measured *via* the voltage produced by the gauge crystal. Due to thermal expansion effects, the length,  $L$ , of the specimen was reduced as needed with increasing temperature until the drive-gauge-rod-specimen period,  $\tau_{DGQS}$ , was within 5% of the drive-gauge period,  $\tau_{DG}$ , meaning conditions were close to ideal resonance. The elastic modulus of the specimen was calculated using the following equation:

$$E = \frac{(4\rho L^2)}{\tau_s^2} \quad (\text{Eq 1})$$

where  $\rho$  is the density and  $\tau_s$  is the period of the specimen. Variation of the value of the gauge voltage,  $V_g$ , provided a range of strain amplitudes. This allowed the investigation of the vibration damping,  $Q^{-1}$ , characteristics of the specimen as a function of strain amplitude. The damping was obtained using

$$Q^{-1} = \frac{2(N\tau_s)^2 V_d}{m_s C_m \pi V_g} \quad (\text{Eq 2})$$

where  $N$  is the transformer ratio for quartz,  $m_s$  is the specimen mass,  $C_m$  is the capacitance of the gauge circuit,  $V_d$  is the voltage

of the drive crystal, and  $V_g$  is the voltage of the gauge crystal. Other details of the PUCOT are given elsewhere.<sup>[3,4,5]</sup>

### 3.2 Metallographic Examination

Small sections were taken from two different specimens. One section represented the material as it was received, and the other specimen represented the material after experiencing 30 min of exposure to a temperature of 865 °C. Figure 2 shows the optical images taken of specimens at a high magnification. The white particles are composed of intermetallic  $\text{MoSi}_2$ , and the black area is the ceramic  $\text{Si}_3\text{N}_4$ .

## 4. Results and Discussion

Microhardness measurements were performed using a Vickers hardness machine. The Vickers hardness numbers for the two

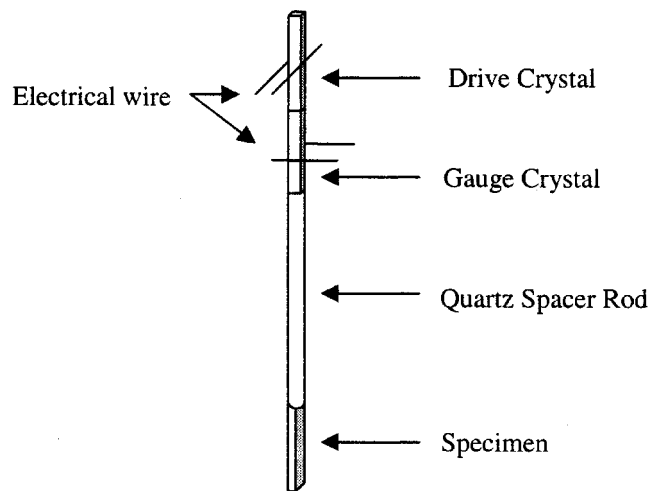
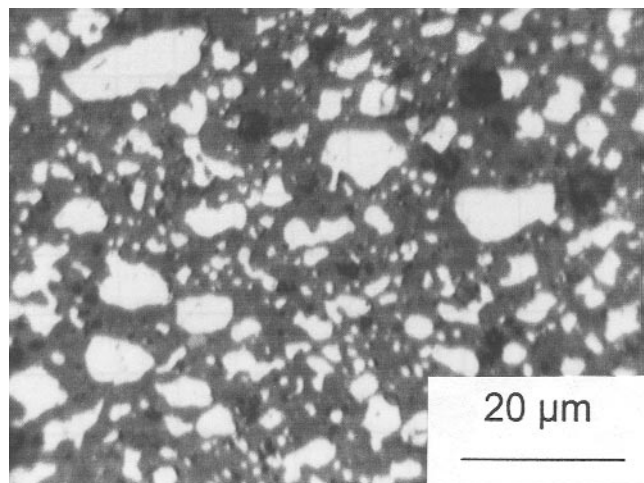


Fig. 1 High-temperature PUCOT setup



(a)

types of phases seen in Fig. 2 are listed in Table 1. The mean hardness values for the dark, ceramic dominant areas were higher than those for the lighter, intermetallic regions. It is also apparent that the dark regions had a higher standard deviation than the light regions. This was due to the dispersion of fine  $\text{MoSi}_2$  particles within the  $\text{Si}_3\text{N}_4$ . The light regions were consolidated phases of intermetallic, while the dark regions were a variable combination of intermetallic and ceramic particles. Particle sizes varied from 1 to greater than 20  $\mu\text{m}$ .

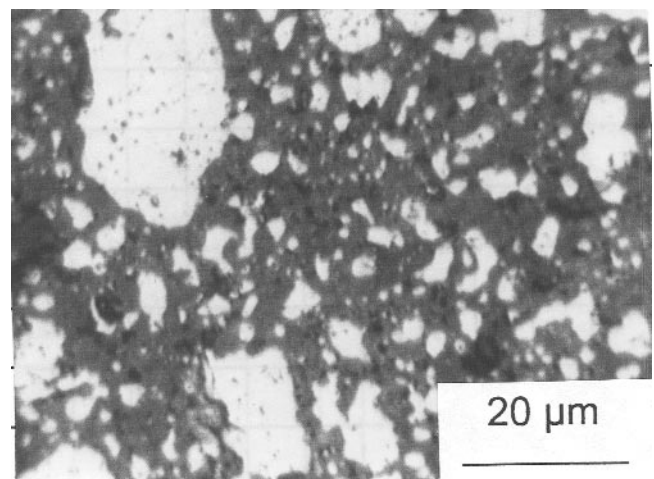
Table 2 summarizes Young's modulus measurements with respect to temperature. These data are also plotted in Fig. 3. Table 3 lists the measured values of mechanical damping over the same temperature range, and Fig. 4 is a plot of the damping versus inverse temperature.

At room temperature,  $\text{MoSi}_2$ -30% $\text{Si}_3\text{N}_4$  displayed an elastic modulus of 290 GPa, which did not correspond with the value of 360 GPa estimated from the rule of mixtures using values for hot isostatically pressed  $\text{Si}_3\text{N}_4$ . Porosity was not accounted for in the estimations and may help to explain some of the difference. From Fig. 3,  $(1/E_0)(dE/dT) = -1.01 \times 10^{-4} \text{ K}^{-1}$ . For ceramics, this value is near  $1 \times 10^{-4} \text{ K}^{-1}$ , while for metals, it ranges between  $4 \times 10^{-4} \text{ K}^{-1}$  and  $14 \times 10^{-4} \text{ K}^{-1}$ .<sup>[6,7]</sup>

The slope of the curve in Fig. 4 is notably different for the room temperature to 240 °C temperature range than it is for temperatures

Table 1 Vickers microhardness 200 g/10s

	Specimen			
	As-received HV		Heat-treated HV	
	Light phase	Dark phase	Light phase	Dark phase
	766.2	941.2	732.6	873.9
	719.7	1083.6	745.8	869.7
	759.3	1011.3	806.0	995.6
	769.7	845.0	853.1	980.3
	759.3	817.4	759.3	904.4
Mean	754.8	939.7	779.4	924.8
Standard deviation	20.15	111.5	49.7	59.4



(b)

Fig. 2 Microstructure of the specimens (a) as received and (b) heated to 865 °C

**Table 2 Dynamic Young's modulus versus temperature**

Temperature, °C	<i>E</i> , MoSi <sub>2</sub> -30%Si <sub>3</sub> N <sub>4</sub> , GPa
21	289.8
240	291.3
340	288.1
450	285.8
595	287.0
800	262.4
865	264.2
970	269.8
Overall change, <i>dE/dT</i>	-0.030

**Table 3 Damping versus temperature**

Temperature, °C	Average <i>Q</i> <sup>-1</sup> , MoSi <sub>2</sub> -30Si <sub>3</sub> N <sub>4</sub>
21	2.63 × 10 <sup>-4</sup>
240	4.08 × 10 <sup>-4</sup>
340	7.87 × 10 <sup>-5</sup>
450	2.11 × 10 <sup>-4</sup>
595	4.56 × 10 <sup>-4</sup>
800	6.33 × 10 <sup>-4</sup>
865	8.44 × 10 <sup>-4</sup>
970	4.61 × 10 <sup>-3</sup>

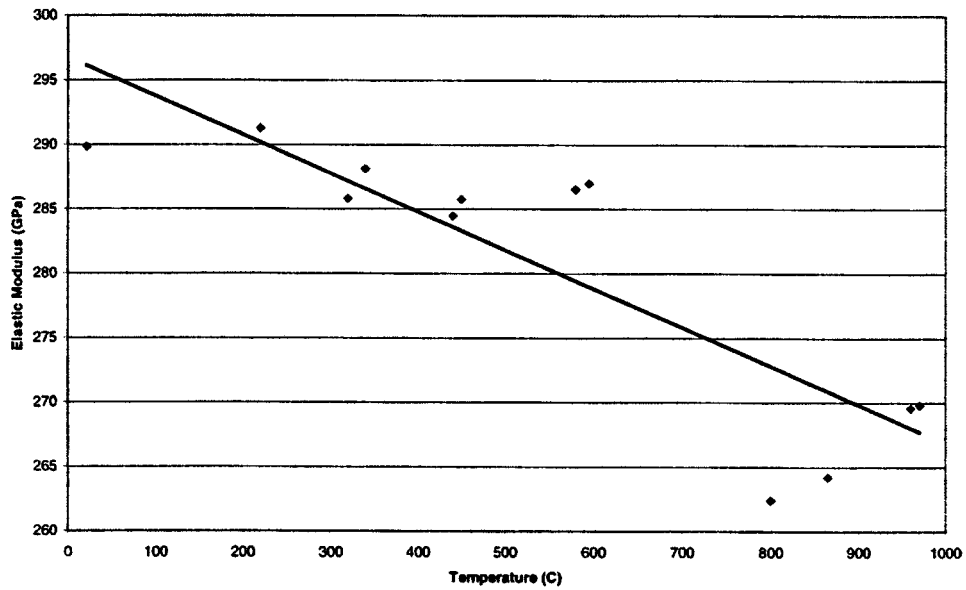


**Fig. 3 Dynamic Young's modulus vs temperature**

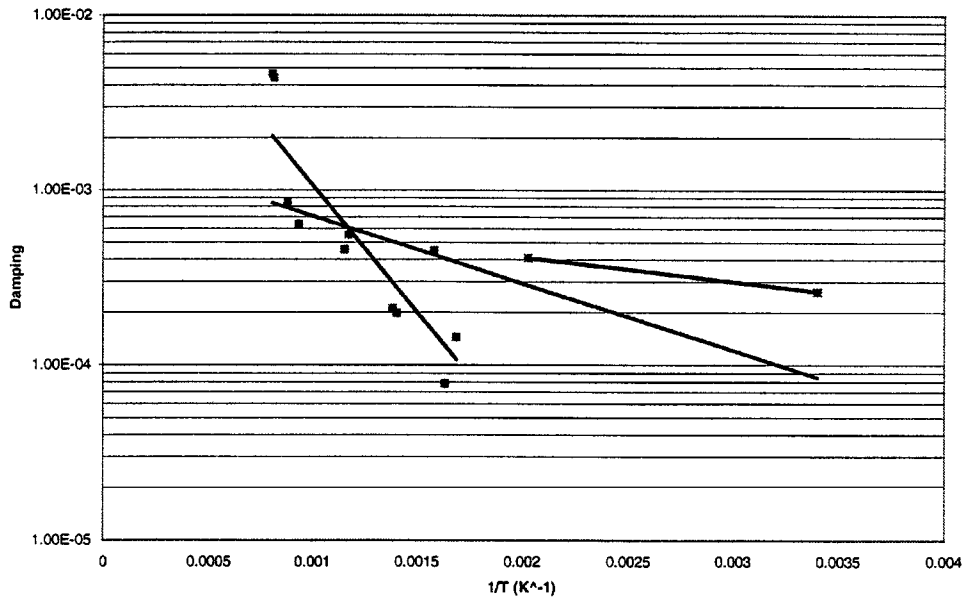


**Fig. 4 Damping vs inverse temperature**

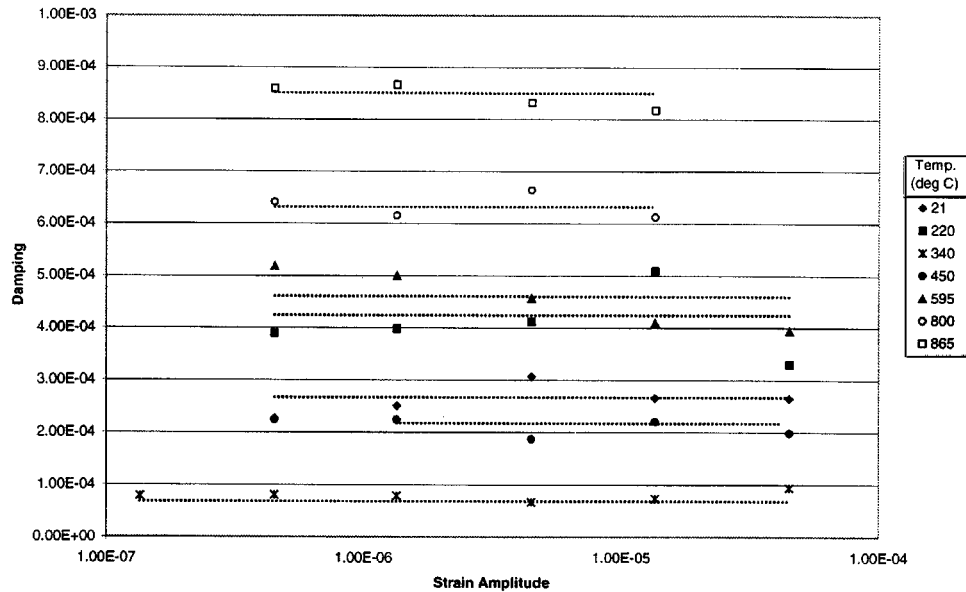


Fig. 5 Damping vs strain amplitude

between 340 and 970 °C. The first two data points resulted in an activation energy of 0.0275 eV/atom, which is close to value for background thermal energy,  $kT$ , where  $k$  is Boltzmann's constant. The remaining data indicate an activation energy on the order of 0.289 eV/atom—over ten times higher. Taken all together, the effective activation energy was 0.0762 eV/atom. Diffusion data on  $\text{MoSi}_2$  are scarce, so it is difficult to check the validity of the measured activation energies. In general, though, these activation energies were low for ceramics. For example, the activation energy for the diffusion of carbon in SiC is near 8 eV/atom.<sup>[8]</sup> Mechanical damping values were approximately independent of strain amplitude in  $\text{MoSi}_2$ -30% $\text{Si}_3\text{N}_4$ , as seen in Fig. 5.

## 5. Conclusions

The following conclusions can be drawn.

The microstructure of  $\text{MoSi}_2$ -30% $\text{Si}_3\text{N}_4$  consisted of varying particle sizes. Particles ranged in size from about 1  $\mu\text{m}$  to greater than 20  $\mu\text{m}$ . The  $\text{Si}_3\text{N}_4$  formed a matrix around the  $\text{MoSi}_2$  particles. The microhardness of the material depended on the size and concentration of  $\text{MoSi}_2$  particles in the region.

The elastic modulus of  $\text{MoSi}_2$ -30% $\text{Si}_3\text{N}_4$  decreased from 289.8 GPa at room temperature to around 269 GPa at 970 °C. Linear regression exhibited a slope,  $dE/dT$ , of  $-0.03$  GPa/K. The normal-

ized modulus,  $E_0^{-1} \times dE/dT$ , was found to be  $-1.01 \times 10^{-4} \text{ K}^{-1}$ . This was in excellent agreement with the approximate value of normalized modulus for ceramics, which is  $-1 \times 10^{-4} \text{ K}^{-1}$ .

Damping in  $\text{MoSi}_2$ -30% $\text{Si}_3\text{N}_4$  was observed to increase with increasing temperature. Average damping at room temperature was  $2.6 \times 10^{-4}$ , while at 970 °C, it was  $4.6 \times 10^{-3}$ . While two distinct regimes were noted in the plot of damping versus inverse temperature, the overall average effective activation energy was found to be 0.0762 eV/atom.

## References

1. M.G. Hebsur: *Mater. Res. Soc. Symp. Proc.*, 1994, vol. 350, p. 177.
2. M.G. Hebsur and M.V. Nathal: *NASA Technical Memorandum 107471*, NASA, Washington, DC, Sept. 1997.
3. J. Marx: *Rev. Sci. Instrum.*, 1951, vol. 22, p. 503.
4. W.H. Robinson and A. Edgar: *IEEE Trans. Sonics Ultrasonics*, 1974, vol. SU-21, p. 98.
5. M. R. Harmouche and A. Wolfenden: *J. Test. Eval.*, 1985, vol. 13, p. 424.
6. *Mechanical and Thermal Properties of Ceramics*, Special Publication 303, J.B. Wachtman, Jr., ed., National Bureau of Standards, Gaithersburg, MD, May 1969, p. 158.
7. J. Friedel: *Dislocations*, Pergamon Press, Elmsford, NY, 1964, pp. 454-57.
8. J. Hong and R. Davis: *J. Am. Ceram. Soc.*, 1980, vol. 63, p. 546.